The Impact of Molecular Crowding on Translational Mobility and Conformational Properties of Biological Macromolecules

Niklas O. Junker[1], Farzaneh Vaghefikia[1], Alyazan Albarghash[1], Henning Höfig[1,2], Daryan Kempe[1,†], Julia Walter[1], Julia Otten[3], Martina Pohl[3], Alexandros Katranidis[2], Simone Wiegand[4,5], Jörg Fitter [1,2,*]

[1] RWTH Aachen University, I. Physikalisches Institut (IA), Aachen, Germany
[2] Forschungszentrum Jülich, Institute of Complex Systems ICS-5, Jülich, Germany
[3] Forschungszentrum Jülich, IBG-1: Biotechnology, Jülich, Germany
[4] Forschungszentrum Jülich, Institute of Complex Systems ICS-3, Jülich, Germany
[5] Universität zu Köln, Physikalische Chemie, Köln, Germany

† present address: The University of New South Wales, Lowy Cancer Research Centre, Sydney, Australia

*Correspondence should be addressed to J.F. (fitter@physik.rwth-aachen.de; phone: +49 241-80-27209).

ABSTRACT

Effects of molecular crowding on structural and dynamical properties of biological macromolecules do depend on the concentration of crowding agents, but also on the molecular mass and the structural compactness of the crowder molecules. By employing fluorescence correlation spectroscopy (FCS) we investigated the translational mobility of several biological macromolecules ranging from 17 kDA to 2.7 MDa. Polyethylene glycol and Ficoll polymers of different molecular masses were used in buffer solutions to mimic a crowded environment. The reduction in translational mobility of the biological tracer molecules was analyzed as a function of crowder volume fractions and was generally more pronounced in PEG as compared to Ficoll solutions. For several crowding conditions we observed a molecular sieving effect in which the diffusion coefficient of larger tracer molecules is reduced to a larger extend than predicted by the Stokes-Einstein relation. By employing a FRET-based biosensor, we also showed that a multi-protein complex is significantly compacted in the presence of macromolecular crowders. Importantly, with respect to sensor *in vivo* applications, ligand concentration determining sensors would need a crowding specific calibration in order to deliver correct cytosolic ligand concentration.

INTRODUCTION

Most of our general knowledge in the field of protein biochemistry stems from experiments with highly diluted proteins in buffer solutions with concentrations of a few grams per liter. These conditions are very different to those that are present in living cells. The cellular cytoplasm is enriched with a wide variety of macromolecules, for example proteins, polynucleotides and cellular organelles. These can make up as much as 10-30 % of the cell volume [1, 2], which results in concentrations of a few hundred grams per liter known as molecular crowding. The resulting "excluded volume" effect can lead to an increase in the effective concentrations of cellular proteins and change physical key properties of the solution and the molecules therein[3, 4]. Accordingly, the proteins' molecular mobility and dynamics can be reduced in these confined volumes, which is generally present in the cytosol[5, 6]. Possible consequences of this molecular crowding are reduced diffusion coefficients, shifts in the balances of protein-protein and protein-substrate associations, and changes in conformational dynamics of individual proteins[2, 7, 8]. In the past several studies on quantifying specific protein properties directly in the cellular cytoplasm have produced numerous valuable insights, as discussed in some recent reviews[6, 9, 10]. However, obtaining information from the cellular interior is often difficult, since experimental access to living cells is not straightforward. A common alternative approach is to mimic various properties of molecular crowding in the cell by buffer solutions with high concentrations of synthetic crowding agents such as the polymers polyethylene glycol (PEG), Ficoll, or dextran or of purified proteins, like lysozyme, bovine serum albumin, or ovalbumin[11]. In particular aspects of translational and rotational diffusion of proteins under crowded conditions have been performed by such *in vitro* crowding studies[12-18]. In this respect, the utilized crowding agents have to meet mainly two major criteria. (i) They should be inert, resulting in minimal chemical interactions with the target molecule and (ii) they should be highly soluble in aqueous buffers. Although the obtained crowded

solutions (*in vitro* studies) do not completely mimic all properties of the cytosolic environment (*in vivo* studies), they provide a well-controllable environment since parameters like concentration, size, shape, diffusivity, and composition of crowding agents can be varied systematically[1, 11, 19].

In this work, we investigated the translational diffusion and the conformational changes of various biological macromolecules as a function of different crowding conditions. These properties represent crucial parameters for almost any cellular process and by this regulate activities in living cells. Translational diffusion of biological macromolecules, used as tracers in crowded environments, was investigated mainly by fluorescence recovery after photo-bleaching (FRAP),fluorescence correlation spectroscopy (FCS) and NMR[13, 15, 16, 20-22]. Several *in vitro* studies showed that crowding based on solutions of highly concentrated proteins differ considerably compared those of highly concentrated synthetic polymer crowding agents. Another important property of macromolecular crowding is given by the fact, that the relative size of the crowder molecules and the biological tracer molecules, typically proteins, has a strong impact of the diffusion of the tracer molecules[15, 18, 20]. Here we present a comparative translational diffusion study using FCS on macromolecular tracer molecules with different sizes and shapes. In focus was to investigate the diffusion of tracer molecules in concentrated PEG and Ficoll solutions with varying hydrodynamic dimensions (i.e. hydrodynamic radii of polymer coils) of the crowder molecules. In this study we prefer to use synthetic polymer crowders since they neither produce significant fluorescence background in FCS measurements, nor they do show the presence of aggregates, even at elevated crowder concentration. For homogenous crowding solutions (using only one type of crowding agent at a time) we were able to reduce artifacts[23] to a minimum, due to the application of state-of-the-art confocal fluorescence detection procedures, which we reported recently[24]. For some representatives of a cytosolic macromolecule we investigated the

translational diffusion of several proteins with sizes ranging from 17kDa to 150 kDa, of a double stranded DNA (31.6 kDa), and of 70S ribosomes (2.7 MDa) under various crowding conditions. Here, ribosomes are of specific interest, since they occupy up to 50% of the cellular volume of *E. coli* and contribute with ~ 10^4 copies per cell[25]. In addition, we also measured the translational mobility of some crowder coils at different crowder concentrations. We compared our results to those obtained from measurements of diffusing tracer molecules in cells[6] and found similarities in the size-dependence of tracer diffusion for some crowder agents[22, 26]. Such a comparison intends to identify crowder agents and *in vitro* crowding conditions that can mimic *in vivo* crowding conditions most appropriate. In addition to translational mobility we monitored the effect of different crowding conditions on the structural compactness of a flexible multi-protein complex. A well-suited system to investigate this aspect is given by FRET-based biosensors which are equipped with fluorescent proteins (FP)[27]. Often these sensors are employed directly in cells or in cytosolic solutions, in both cases heavily affected by the crowding properties[28], amongst others[29]. Here, we investigated a glucose sensor showing glucose-induced conformational changes which take place concurrently with crowder induced compaction of the sensor structures. The results indicate that the crowder induced compaction overlays the glucose induced FRET-effect and challenges the application of such sensors for quantitative measurements *in vivo*.

EXPERIMENTAL SECTION

Sample preparation. In addition to a small crowder molecule, namely glycerol (M_w: 92.1 Da) we employed two types of artificial macromolecular crowder molecules (Fig. S1). Ficoll is a highly branched synthetic co-polymer of saccharose and epichlorhydrine which forms soft but compact spheres in aqueous buffers. We used Ficoll 70 (M_w: 70 kDa; GE Healthcare, Munich, Germany) and Ficoll 400 (M_w: 400 kDa; Sigma-Aldrich, Taufkirchen, Germany). Besides, polyethylene glycol (PEG) or polyethylene oxide (PEO), a linear non-branched polymer chain forms coils or

more expanded particles in aqueous buffers than Ficoll at the same molecular weight[30, 31]. In this study we used PEG35 (M_w: 35 kDa), PEO100 (M_w: 100 kDa), PEO200 (M_w: 200 kDa) and PEO300 (M_w: 300 kDa), all from Sigma-Aldrich, Taufkirchen, Germany. All buffer solutions (50 mM HEPES, pH: 7.2, or Tico buffer for crowding solutions with ribosomes, see below) containing glycerol as well as Ficoll were prepared by stirring for 18 h at 35 °C and finally stored at 4 °C, while PEG/PEO containing solutions were prepared by shaking the solutions for 30 minutes and finally storing them at room temperature. Crowder volume fractions ϕ were calculated for crowder solutions by using partial specific volumes of 0.65 and 0.83 mL/g for Ficoll and PEG solutions, respectively[32]. For studies investigating self-crowding, we employed PEG35 and Ficoll70 fluorescently labelled with Cy5 which was purchased from Nanocs Inc., Boston, USA. Labeled polymers were added to the respective unlabeled crowder solution in nanomolar concentrations in order to perform FCS studies.

Macromolecular tracer molecules were characterized by different molecular weight, different molecule size, and by different molecule shape (see Fig. S2). For the following macromolecules used in this study we measured first the hydrodynamic radius R_H in aqueous buffers (50 mM HEPES, pH: 7.2) by FCS. Calmodulin (M_w: 17 kDa, R_H: 2.6 nm, dumbbell shaped, labelled with Alexa 647, labeling procedure described previously[33]), Green fluorescence protein, GFP (M_w: 27 kDa, R_H: 2.8 nm, barrel shaped, intrinsic fluorophore, protein synthesis described previously[34]), Streptavidin (M_w: 60 kDa, R_H: 3.2 nm, compact oblate ellipsoidal structure, Alexa 488 labeled protein purchased from Thermo Fisher, Karlsruhe, Germany), double stranded DNA of 48 base pairs (M_w: 31.6 kDa, R_H: 3.9 nm, cylinder of 2 nm width and 16 nm length, labelled with Alexa 647, sample preparation and labeling procedure described previously[35]), and Immunoglobulin G (M_w: 150 kDa, R_H: 6.0 nm, Y-shaped, Alexa 488 labeled protein purchased from abcam, Cambridge, UK). Ribosomes (M_w: 2.7 MDa, R_H: 12.8 nm, compact spherical structure) from *E.coli* were produced, purified, and labelled as described in Ref. [34]. Briefly, cells of the RNase deficient *E. coli* K-12 strain CAN20/12E were grown at 37 °C and incubated on ice for 1 h before harvesting. Ribosomes were isolated by sucrose gradient centrifugation using a zonal rotor and resuspended in Tico buffer [20 mM Hepes-KOH (pH 7.6 at 0 °C), 10 mM magnesium acetate, 30 mM ammonium acetate, 4 mM β-mercaptoethanol]. For labelling, purified ribosomes reacted with a Cy5-NHS-ester (GE Healthcare Life Sciences, Little Chalfont, UK) in labeling buffer [50 mM Hepes-KOH (pH 7.5), 10 mM $MgCl_2$, 100 mM KCl] for 20 min at 37 °C, using a 20-fold

excess of dye to minimize the unlabeled fraction of ribosomes. The excess of dye was removed by pelleting the ribosomes through a 1.1 M sucrose cushion. After resuspending the pellet in Tico buffer, aggregates were removed by centrifugation and the aggregate-free supernatant was used for further experiments. In average each 70S ribosome particle was labelled with five to six Cy5-dyes. Fluorophores used for own labeling procedures were purchased by Thermo Fisher Scientific, Karlsruhe, Germany. The employed glucose sensor construct is based on the composition of a glucose binding protein flanked by two fluorescent proteins (FPs) as introduced by Deuschle et al. (sensor FLII12Pglu 600μ)[36], but carries improved FP variants (ECFP for donor FP and Citrine for acceptor FP). The respective sequence and details on sensor production and sample preparation are given in previous publications[29, 37]

Sample characterization. The refractive indices of all solutions were determined using an Abbe refractometer (A. Krüss Optronic, Hamburg, Germany). Macroscopic viscosities of crowder solutions were determined by using a Falling Sphere Viscometer (AMVn Automated Microviscometer and a LOVIS 2000 M Microviscosimeter, both Anton Paar, Ostfildern-Scharnhausen, Germany) and a Density Meter (DMA 4500 Density Meter, Anton Paar, Ostfildern-Scharnhausen, Germany). Absorption spectra of fluorescently labelled molecules were recorded using a Shimadzu (Kyoto, Japan) UV-2600 double-beam UV-VIS spectrophotometer. Fluorescence emission spectra were measured on a spectrofluorometer (Quanta Master 40, Photon Technology International, Birmingham, USA).

Biosensor FRET measurements. The intensity ratio $R = I_A/I_D$ derived from the respective fluorescence emission intensities (I_A from the acceptor and I_D from the donor fluorophore) is related to the ligand concentration (here: D-glucose). This ratio exhibits a minimal value (R_{apo}) for the non-liganded state of the sensor and a maximal value (R_{max}) for the fully saturated sensor molecule. Isothermal titration curves of the glucose sensor were determined in a microtiter plate spectrofluorimeter as described earlier[37]. Per well, 50 µl of sensor solution was mixed each with 50 µl of 13 different D-glucose solutions (20 mM MOPS, pH 7.3, final glucose concentrations 1 µM – 0.1 M). The quotient *R* of acceptor and donor peak intensities was plotted as a function of the glucose concentration [G] and fitted with a sigmoidal curve

$$R = \left(R_{max} - R_{apo}\right)\frac{[G]}{K_D+[G]} + R_{apo} \quad (1)$$

where R_{apo} is the ratio without glucose, R_{max} is the ratio at saturated glucose concentrations, and K_D is the glucose concentration at which *R* increased to half of its maximal rise. The sensitivity of

sensors is typically characterized by $\Delta R = R_{max} - R_{apo}$. Larger ΔR-values represent higher sensor sensitivities.

Confocal microscopy. Fluorescence Correlation Spectroscopy (FCS) and time-resolved anisotropy (TRA) measurements were performed with a commercial confocal microscope (MicroTime200, Picoquant, Berlin, Germany) equipped with a red (633nm) and a blue (481nm) diode laser and an UPLSAPO 60x/1.2NA objective from Olympus (Shinjuku, Japan). The emitted fluorescence photons were collected by the microscope objective and passed through a dual-band dichroic mirror (Omega 475-625DBDR, Brattleboro, USA). Subsequently, they were focused on a 30 μm pinhole and splitted into two detection channels, either by a 50/50 beam splitter cube (for FCS) or by a polarizing beam splitter cube (for TRA), both from Linos Photonics (Göttingen, Germany). The red photons filtered by a bandpass emission filter (Chroma Technology HQ690/70M) and the blue photons filtered by a bandpass emission filter (Omega Optical XF 3003 520DF40) were detected by two silicon avalanche photodiodes (τ-SPAD). The lasers are operated at a frequency of 20 MHz by means of a computer controlled PicoQuant PDL828 Sepia-II laser driver. Photon counts are processed with a "PicoHarp-300" time correlated single photon counting (TCSPC) acquisition unit from PicoQuant.

FCS curves were generated and analyzed with the help of the software SymphoTime64 from PicoQuant (see ref.[24] for more details). Time-resolved anisotropy (TRA) was analyzed with self-written Matlab (Mathworks, Nattick, USA) routines (for details see[38]). For the FCS studies we employ labelled molecules at sample concentrations in the nanomolar regime. As demonstrated in a recent study[24] FCS artifacts due to refractive index mismatch caused by crowder solutions with refractive indices up to 1.4 can be reduced best by the following instrumental settings: (i) a short distance of the confocal volume from the cover slide surface (~ 10 μm) and (ii) a small confocal pinhole (diameter 30 μm). To circumvent depolarization effects stemming from the use of high NA objectives, time-resolved anisotropy measurements are performed using an Olympus UplanFl 10x/0.3NA objective. All other data-sets were processed with Origin Pro (Northampton, USA).

RESULTS AND DISCUSSION

Properties of concentrated crowder solutions

Before we investigated the impact of molecular crowding on the mobility of different biological tracer molecules in detail, some properties of the crowding agents in buffer solutions were characterized. Since the polymer crowder agents used in this study are assumed to form more or less densely packed coils or particles in aqueous solutions, we first measured the translational diffusion of fluorescently labeled Ficoll70 and PEG35 (see Experimental Section), highly diluted in aqueous buffer. The obtained diffusion coefficients exhibit a rather broad distribution (Fig. 1a,b). For the PEG35 and Ficoll70 solutions the obtained mean values of the diffusion coefficient (see legend Fig. 1) correspond reasonable well to the calculated hydrodynamic radii as given in Fig. S1. The rather broad distribution of diffusion coefficients of polymer coils is most probable related to a certain distribution in the molecular mass of the polymer chains and to a size distribution of formed random coils (i.e., polydispersity). In contrast, the diffusion of rigid-body-like proteins, such as streptavidin, shows a much narrower distribution of diffusion coefficients (Fig. S3). In the next step we measured the translational diffusion of the fluorescently labeled crowding agents in the presence of the same non-labeled crowder molecules, the latter in high concentrations. In this way the translational mobility of a few labeled crowder molecules represents the mobility of all crowder molecules, also of the non-labelled ones, which cause the crowding (self-crowding). Based on the diffusion properties determined in pure buffer solutions, we could measure the reduction of the related diffusion coefficients in solutions with increasing crowder concentrations (Fig. 1c,d). At a crowder concentration of approximately 2.5 mM, which corresponds to an apparent crowder volume fraction $\phi \sim 0.1$, the diffusion reached its lowest value with $D \sim 5\ \mu m^2/s$ (see Fig. S4a,b).

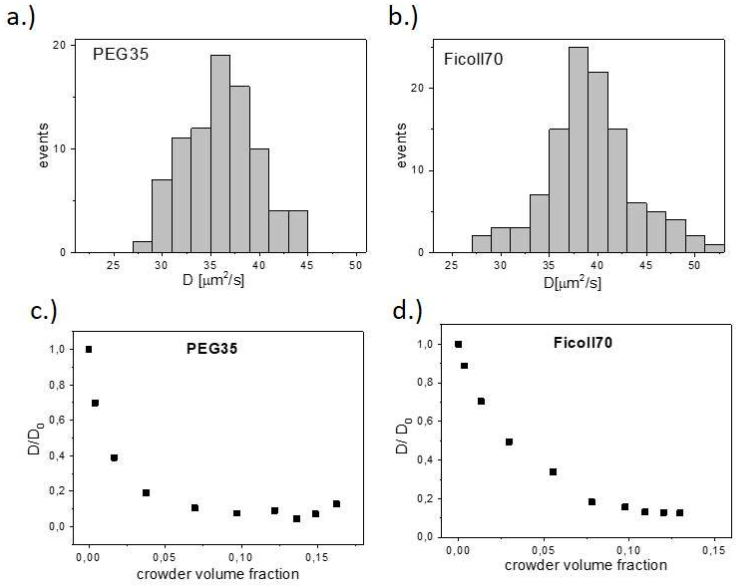

Fig. 1: *Distribution of diffusion coefficients from repetitive FCS measurements were obtained for polymer crowders PEG35 (a) and Ficoll70 (b) in highly diluted aqueous buffer solutions. The obtained mean D-value of 36 μm²/s for PEG35 and 38 μm²/s for Ficoll70 correspond to R_H-values of 5.7 nm for PEG35 and 5.6 nm for Ficoll70, respectively, (using the Stokes-Einstein equation, see eq. 3a). Furthermore, translational diffusion of labeled polymer crowder molecules were measured as a function of crowder volume fraction (self-crowding) for PEG35 (c) and for Ficoll70 (d).*

To our surprise, at concentrations larger than ~2.5 mM we observed diffusion coefficients above zero. This is most probably caused by an artifact of the FCS measurements. Very slow diffusing (for example caused by collective diffusion together with a polymer mesh) or even immobile fluorescently labelled polymer particles experience photo-bleaching after a certain time. Obviously this caused a fluctuating signal in the measured time trace, which is interpreted as translational diffusion in the FCS analysis and practically results in overestimated diffusion coefficients[34]. This assumption is supported by the observation that the diffusion coefficients show smaller values for lower laser excitation power at concentrations above ~2.5 mM (Fig. S4a,b). However, the interpretation of the observed reduced diffusion of crowding agents at higher concentrations (here

for example above ~2.5 mM) is not straightforward. At least two major aspects must be considered in the semi-diluted and concentrated regime. (i) Most polymer samples are generally prone to form larger aggregates, caused by intermolecular entanglement[39, 40]. This would lead to a scenario better characterized by a polymer mesh instead of individual mobile single chain coils or particles. (ii) The hydrodynamic radii, typically obtained for the various polymer crowding agents in the diluted regime, would most probable show slightly smaller values when the intermolecular interactions become more dominant at higher concentrations and may cause a certain compaction[41]. We assume that in particular for the flexible PEG crowding agents the polymer particle size decreases with the crowder concentration. However, within the scope of the present work we did not consider possible variations of R_H-values as a function of the polymer concentration. Instead we utilize published R_H-values for Ficoll70 and PEG35 polymer coils (see Figure S1 and ref.[30, 31]). Based on this information the R_H values of Ficoll70 and PEG35 are rather similar (5.1 and 5.7 nm, respectively). The overlap concentration for flexible polymer is given by[18]

$$c^* = \frac{M_w}{4/3 \cdot \pi \cdot R_g^3 N_A} \tag{2}$$

where R_g is the radius of gyration of the polymer particle. We obtain overlap concentrations which are 2.14 mM and 2.98 mM for PEG 35 and for Ficoll 70, respectively. Specifically, in this semi-dilute concentration regime the disappearance of any self-diffusion of polymer coils or particles was observed.

In comparison to reduced crowder molecule mobility under crowding conditions the translational diffusion of a protein (streptavidin) under the same conditions was analyzed. Despite the structural differences between the flexible polymer coils or particles and the more rigid streptavidin structure, we observed a rather similar reduction of the translational mobility of tracer molecules

in the respective crowding solutions. This is exemplarily shown for streptavidin in Ficoll70 and in PEG35 where D/D_0 is plotted as a function of the molar crowder concentration (Fig. S4c,d).

Mobility of biological macromolecules in crowded solutions

It is already known from previous studies that the translational mobility of biological tracer molecules does not only depend on the concentration of the macromolecular crowder solutions, which is typically related to the macroscopic viscosity η of the crowder solution. Also the relative size between polymer crowder coils or particles and the biological tracer molecule matters[15, 18]. Diffusion coefficients of tracer molecules were measured as a function of crowder concentrations for which we determined the respective macroscopic viscosities (see Fig. S5). According to the Stokes-Einstein equation (eq. 3a) and the Stokes-Einstein-Debye equation (3b), the translational and the rotational diffusion coefficient (D^t and D^r, respectively) should be inversely proportional to the viscosity.

$$D^t = \frac{k_B T}{6\pi\eta R_H} \tag{3a}$$

$$D^r = \frac{k_B T}{8\pi\eta R_H^3} \tag{3b}$$

However, we observed a clear deviation from the Stokes-Einstein predictions for translational and rotational diffusion. This is shown exemplarily for the double stranded DNA diffusing in Ficoll 70 solutions with different concentrations up to 21% [w/w] (see Fig. 2a). By making use of the power law dependence[15]

$$\frac{D_0^{t,r}}{D^{t,r}} = \left(\frac{\eta}{\eta_0}\right)^{q_{t,r}} \tag{4}$$

translational as well as rotational diffusion (with diffusion coefficients D^t and D^r, respectively) of tracer molecules can be described in solutions with macromolecular crowders. Here D_0 and η_0 represent values obtained for pure aqueous buffer solutions and the exponent $q_{t,r} \leq 1$ describes the deviation from the Stokes-Einstein behavior ($q_{t,r} = 1$).

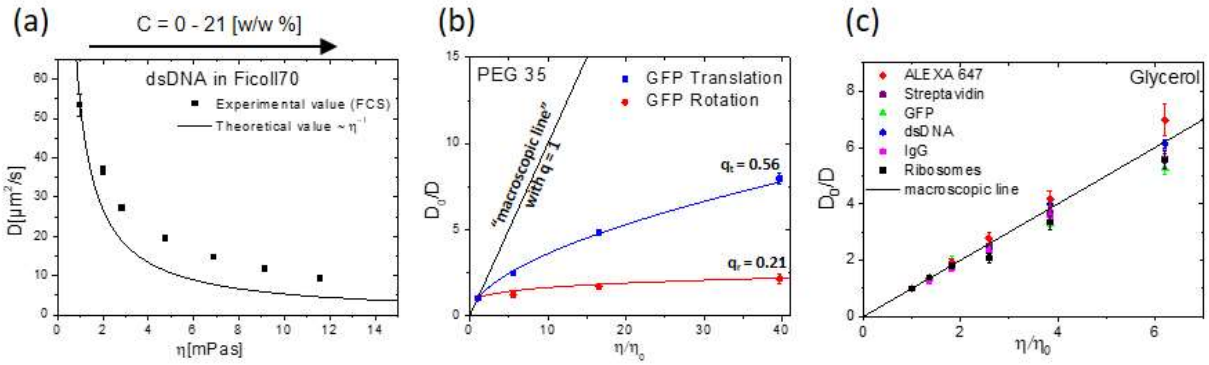

Fig. 2: *(a) Translational diffusion coefficients of dsDNA measured with FCS in solutions with increasing Ficoll70 concentration. The coefficients were plotted as a function of the bulk viscosities as measured for the respective solutions. (b) Translational as well as rotational diffusion coefficients of GFP in PEG35 solutions were determined by FCS and by time-resolved anisotropy decays, respectively (see Experimental Section). The dependence of D^t and D^r on the bulk viscosity (see eqs. 3a,b) exhibits an even stronger deviation of rotational diffusion from the macroscopic line (q = 1) as compared to translational diffusion. (c) In concentrated solutions with the small crowding agent glycerol the translational diffusion of various macromolecules, of different size (as given in Fig. S2), follows the ordinary Stokes-Einstein behavior (all data points from the Stokes-Einstein prediction fall on the q = 1 line).*

As shown for GFP in PEG35 solutions, the rotational diffusion becomes even more independent of the viscosity than the translational diffusion (Fig. 2b, Fig. S5). These results confirm previous studies which report that diffusing molecules in highly concentrated solutions with macromolecular crowding agents do not fully experience the (macroscopic) bulk viscosity as measured in the falling sphere viscometer[15, 16, 21, 42]. The deviation of the microscopic from the macroscopic viscosity can be parameterized by the q-value, which decreases with increasing deviation ($q_r < q_t \leq 1$)[15]. For crowder molecules, much smaller than the diffusing tracer molecules

(for example glycerol), the assumptions of the Stokes-Einstein equation (i.e. point-like particles which build up the surrounding medium in which a much larger spherical particle diffuses) become applicable. As a consequence, we observed proportionality between translational diffusion coefficient and the bulk viscosity, as shown for various diffusing macromolecular tracer molecules in glycerol solutions in Fig. 2c. All measured values fall on the "macroscopic line" with q = 1. We study the translational diffusion by employing (i) crowding agents, which form more compact particles (Ficoll) or more expanded polymer coils (PEO/PEG) as well as (ii) macromolecular tracer biomolecules, which vary in size and shape (see Fig. S1 and Fig. S2). Plots of relative diffusion coefficients against relative viscosities allowed for determination of the corresponding q-values (for all results see Fig. 3 and Table S1). In a first approach, we analyzed the tracer diffusion in PEG35 and in Ficoll70 solutions. As shown in Fig. 1a,b the employed polymers form collapsed coils with a hydrodynamic radius of 5.7 and 5.6 nm, respectively. These collapsed polymer structures are typically larger (or approximately equal) than the size of the diffusing tracer molecules and we observe a clear deviation from the results obtained for glycerol (see Fig. 2c). Therefore, all obtained data points can be found below the macroscopic line with values of $q < 1$ (Fig. 3a,b and Tab. S1). Interestingly, NMR studies showed, that the use of proteins as crowder agents cause the opposite effect, i.e. with values of $q > 1$, as compared to polymer crowders[17]. However, tentatively the results obtained from both synthetic crowding agents (Ficoll70 and PEG35) indicate, that the deviation from the macroscopic line is controlled by the size relation of crowder and tracer molecules. In a second approach we investigated the tracer diffusion of Streptavidin (spherical shape) and that of the dsDNA (cylindrical shape) in crowder solutions in a systematic manner as a function of the crowder size (Fig. 3c,d). Again at least tentatively a size-scaling behavior was observed with larger q-values for the case that R_H of the crowder molecules

(ranging from 0.31 – 19.4 nm) approaches the values of the tracer molecule (R_H = 3.2 - 3.9 nm). Compared to Streptavidin, dsDNA has generally smaller q-values in particular for the smaller crowder molecules PEG35 and Ficoll70. A similar general behavior was observed earlier and is caused by the failure of hydrodynamics at the microscopic scale[15]. The reason for this is given by the fact that the measured bulk viscosities show much higher values for larger crowding agents compared to smaller ones at a given crowder mass concentration (see Fig. S5).

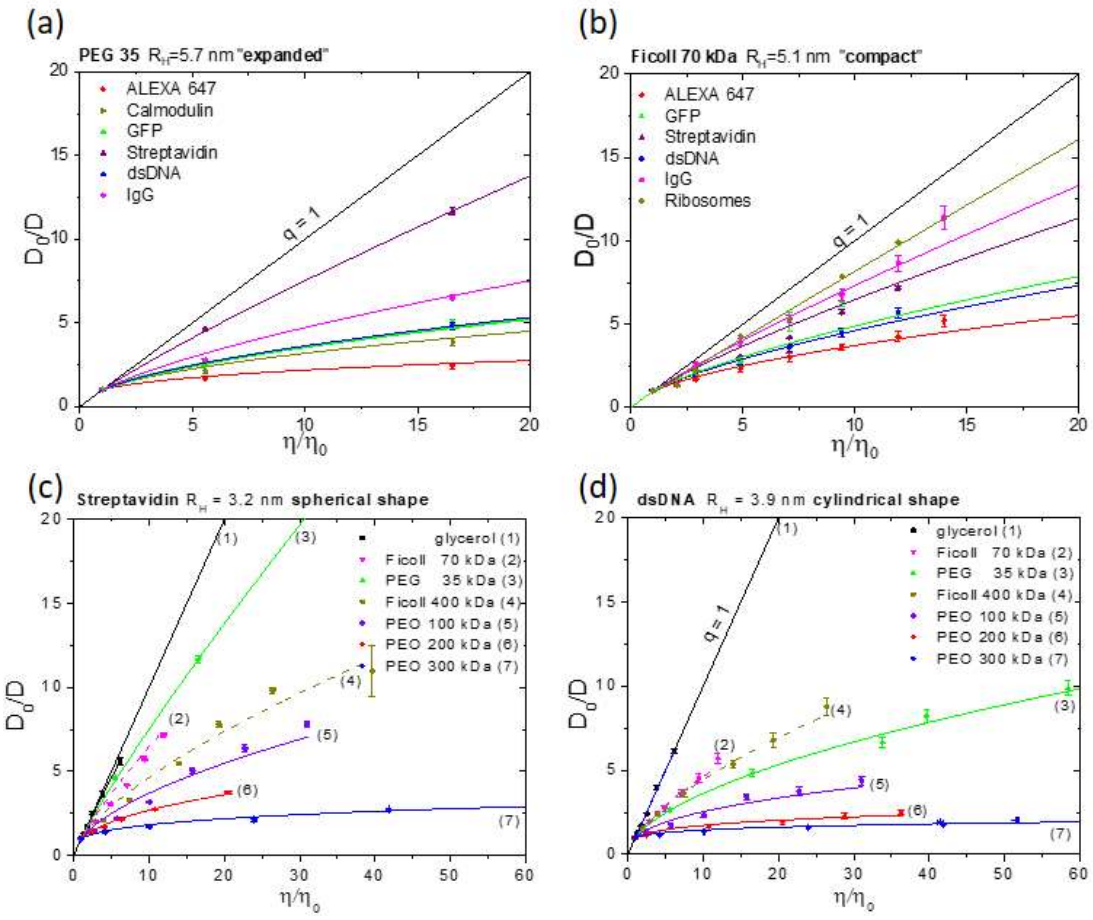

Fig. 3: *Ratios of translational diffusion coefficients versus the ratios of respective bulk viscosities. The upper panels show diffusion properties of various tracer molecules from small (Alexa647-dye) to large (IgG, Ribosome) in PEG 35 (a) and in Ficoll 70 (b). In a similar manner diffusion properties of streptavidin (c) and of dsDNA (d) are shown in crowder solutions with crowding agents from small (glycerol) to large (PEO 300) sizes. Solid (PEG 35) and dashed (Ficoll 70) lines represent fits of the experimental data according to equation 4. The resulting q-values are given in Tab. S1.*

For a better comparison we analyzed the tracer diffusion also as a function of the crowder volume fraction ϕ, which is controlled by the crowder size and the crowder concentration in a given solution. (Fig. 4a-c). A comparison of the relative reduction of translational diffusion (D_0/D) as a function of crowder volume fraction exhibits that PEG crowders in general cause a stronger reduction for the shown tracer molecules as compared to Ficoll crowders. Only for ribosomes, Ficoll 400 exhibits a similar strong reduction like the PEG agents. In addition, the extend of crowder induced reduction of translational diffusion depends on the size of the tracer molecules. This dependency can be described by a simple power law

$$D^t = c \cdot M_w^x \tag{5}$$

where M_w is the molecular mass of the tracer molecule, c is a scaling factor and x gives the exponent which characterizes the reduction of translational diffusion[6, 26]. In pure aqueous solutions we expect an exponent x = - 0.33, a dependency which follows essentially the Stokes-Einstein relationship (see eq. 3a). Such a behavior is reproduced by our data from diffusion in pure aqueous buffer, as shown in Fig. 4d. For a crowder volume faction value of 0.13, which is similar to the corresponding values in prokaryotic cells, we obtained rather different exponent values (Fig. 4d). For Ficoll 70 the absolute diffusion coefficients are reduced in similar manner as compared those obtained by aqueous buffer solutions with an exponent value close to x = - 0.33. In contrast to this, PEG 35, PEG 100 and Ficoll 400 exhibit significantly lager exponent values form - 0.74 to - 1.27. The latter behavior was observed for diffusion of biological macromolecules in the cytoplasm of *E. coli* and was attributed to a molecular sieving effect. Following this picture, the crowded environment appears as mesh network which allows small molecules a relative free diffusion while larger molecules experience a restricted diffusion[9, 26]. Most probable either PEG crowder agents, which have a stronger tendency to from mesh networks, or crowder agents with a sufficient large coil size (here Ficoll 400 in contrast to Ficoll 70) have the ability show this sieving effect.

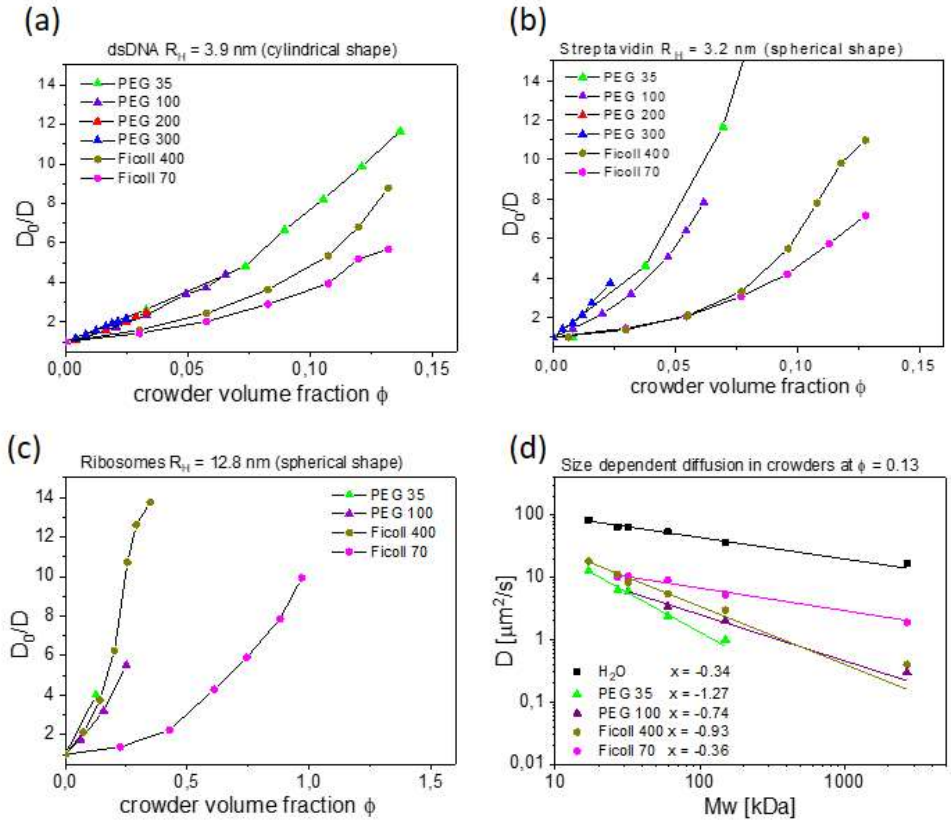

Fig. 4: *Ratios of translational diffusion coefficients for tracer molecules versus crowder volume fraction for dsDNA (a), streptavidin (b) and 70 S Ribosomes (c). (d) The size dependence of tracer diffusion is shown for different crowder agents, but for all solutions with the same crowder volume fraction of $\phi = 0.13$.*

A comparison of absolute diffusion coefficient of GFP and ribosomes, measured here in synthetic crowders (e.g., Ficoll 400 and PEG 35) and in *E.coli* cells[9, 25] at approximately the same crowder volume fraction of $\phi \sim 0.13$, shows that diffusion in synthetic crowders is rather similar for GFP, but still much faster for ribosomes. GFP diffusion (in water $D^t \sim 65$ μm²/s) drops down to 3-14 μm²/s in cells and to ~ 6-10 μm²/s in PEG 35 or in Ficoll 400. In the case of ribosomes, where the diffusion (in water $D^t \sim 17$ μm²/s) shows 0.04 μm²/s in cells and ~ 0.4 - 2 μm²/s in synthetic crowders. This disagreement for ribosomes is most probably caused by the fact that FCS measurements cannot resolve diffusion coefficients orders of magnitude below one μm²/s.

Crowder-induced biosensor compaction

It is well known that macromolecular crowding has not only an impact on translational or rotational mobility of individual bio-macromolecules, but also on the compactness of intrinsically disordered proteins, of multi-domain proteins, or of multi-protein complexes [7, 11, 43]. An effective approach to study conformational properties of bio-macromolecules under crowding conditions is to employ FRET based biosensors [32, 44, 45]. In a similar manner we make use of a FRET biosensor which is based on a glucose binding-protein that is flanked on either end by two fluorescent proteins (FPs) forming a FRET pair. The conformational change in the glucose binding-protein induced by binding of D-glucose is translated into a change in distance and/or orientation of the FRET-partners (a cyan FP as the donor and a yellow FP as the acceptor, see Fig. S6) and results in changes of the FRET ratio. This principle can be used to quantify the glucose concentration by an optical read out [29, 36]. Here, we analyzed the ligand (D-glucose) induced change in FRET in the presence of several crowding agents, which we employed already in the preceding sections. For this purpose, isothermal binding curves of the glucose sensor were measured as a function of the glucose concentration (Fig. 5). Typically, these curves are utilized for the calibration of a sensor and allow to determine glucose concentration in a concentration range where the ratio $R = I_A/I_D$ exhibits a pronounced change (here approximately from 100 μM to 50 mM), see Experimental Section for details. The sensitivity of a certain sensor construct is characterized by the largest possible change of R-values between non-liganded conditions and fully liganded (saturated) conditions (i.e. the value of ΔR, see Experimental Section). In the case of the crowding agent with the lowest molecular mass, i.e. glycerol, we do not observe an impact of crowding on the binding curves (Fig. 5a). In contrast, PEG35 and Ficoll70 have a profound impact on the corresponding binding curves as compared to non-crowding conditions (Fig. 5b,c). A more detailed analysis of

the obtained data for PEG35 and Ficoll70 revealed the following results: (i) For the non-liganded glucose sensor (at glucose concentrations ≤ 1 µM) R-values show constantly increasing values for increasing crowder concentrations (Fig. 5d). Similar to earlier studies on crowding sensors[28, 44], this indicates that both crowders induce a compaction of the sensor construct. (ii) For all employed crowder concentrations we still observe the typical binding curve showing the sigmoidal shape with increasing glucose concentrations. This indicates that besides glucose induced sensor compaction there is an independent additional compaction of the whole sensor construct caused by both crowder agents. On the other hand, crowding agents seems not to compact only the glucose binding-protein, as we have shown recently[46].

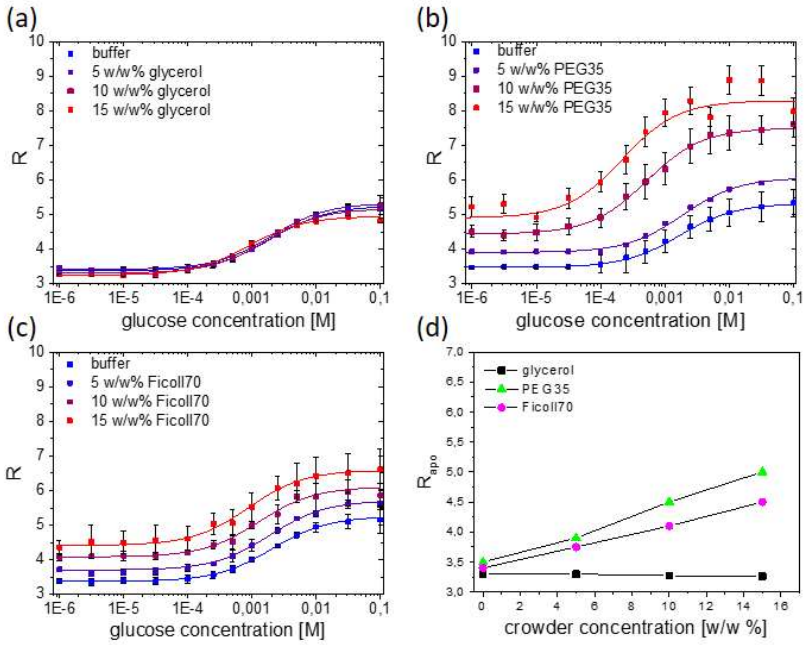

Fig. 5: *The sensor signal R for the FRET-based glucose sensor was measured as a function of the glucose concentration and fitted by an isothermal binding function (colored solid lines according to eq. 1, see Experimental Section). The respective binding curves and the related experimental data (see symbols) are shown for three different crowding agents, glycerol (a), PEG35 (b), and Ficoll70 (c) at crowder concentrations between 0 – 15 % w/w in 20mM MOPS buffer (see Experimental Section). The crowder induced compaction of the non-liganded sensor construct is shown for different crowding agents as a function of crowder concentration (d).*

(iii) Ficoll70 induces a rather uniform compaction of non-liganded and of liganded states, with rather similar K_D-values and ΔR-values for all crowder concentrations (Fig. 5c). The impact of PEG35 seems to be more elaborate. It shows a more pronounced crowder induced compaction (Fig. 5d) and in particular higher crowder concentrations (10-15 w/w%) lead to higher ΔR-values and slightly smaller K_D-values as compared to the non-crowded conditions (Fig. 5b and Fig. S7a). However, the comparison with data as a function of crowder volume fraction exhibits only a moderate difference between Ficoll 70 and PEG 35 (Fig. S7b). Interestingly, our results demonstrate that in principle also a metabolite sensor can be employed as a crowding sensor[47]. In summary we can state that macromolcular crowding has a pronounced impact on the sensor compaction. For this reason the optical readout of FRET-based metabolite sensors in crowded environments needs a calibration under the same environmental condition like the final measurement, if a reliable metabolite quantification is intended[29]. If for example an *in vivo* application in prokaryotes is intendent, crowding conditions with $\phi \sim 0.13$ are suitable for an *in vitro* calibration with PEG 35 as well as with Ficoll 70 (Fig. S7b), as also demonstrated recently for an application with a crowding sensor[28].

CONCLUSION

By making use of a recently developed approach[24] to minimize artifacts in FCS studies mainly caused by refractive index mismatch in additive enriched aqueous solutions, we were able to obtain reliable diffusion coefficients of biological tracer molecules in synthetic polymer crowder solutions at concentrations up to 25 w/w%. In a systematic study with six different macromolecular tracer molecules and seven different crowding agents. First, we analyzed the translational mobility of polymer crowder coils themselves as a function of the crower concentration. The FCS results

showed that the translational mobility of crowder polymer particles decreased in a similar manner as rigid-body like protein tracers (here: streptavidin) under the same crowding conditions. The translational diffusion on the FCS length scale (a few hundred nanometer) comes almost to rest for all macromolecules when the semi-diluted regime is reached, approximately given by the overlap concentration for flexible polymers. Depending on the size of the polymer crowder coils or particles, this concentration is reached between 0.05 mM and 2.5 mM (from large to small crowders). A residual apparent slow diffusion visible in the FCS data is most probable an artifact caused by photo-bleaching effects. However, a fast local diffusion process of tracer molecules in the confined space, effectively built up by the polymer mesh, is still possible [48]. According to the Huggins equation describing the bulk viscosity of concentrated polymer solutions, we obtain much higher viscosity values for larger crowding agents as compared to smaller ones at the same w/w% mass concentration. Therefore, we observed in the case of tracer diffusion that concentrated crowder solutions with larger crowding agents exhibit a much stronger deviation from the "macroscopic line" in D_0/D versus η/η_0 plots as compared to smaller crowding agents. A direct look on the reduction of diffusion coefficients as a function of the crowder volume fraction, revealed that PEG crowders cause the most pronounced reduction of the tracer diffusion. Furthermore, solutions with several crowder agents exhibit a tracer size dependence of the diffusion reduction, which indicates a molecular sieving effect. This effect was also observed in the cytoplasm of cells and seems to be a general property of cellular crowding. With respect to absolute diffusion coefficients we observe a reasonable agreement between measurements in cells and in synthetic crowder solutions for GFP. In the case of very slow diffusion, for example for ribosomes in highly crowded environments, FCS measurements fail to deliver diffusion coefficients below ~ 1 $\mu m^2/s$ with the required accuracy. A more appropriate approach to study

slow diffusion of biological macromolecules in crowded environments is given by single particle tracking methods[49]. In fact, a reliable knowledge about ribosome diffusion, but also about the diffusion of smaller molecules under the same crowding conditions, is of specific interest for elucidating the impact of macromolecular crowding on cellular processes like protein synthesis. In this respect molecular sieving effects and the translational mobility of 30S and 50S subunits, the latter important for the 70S formation, are worth to be studied, for example in cell-free protein synthesis assays[34, 50, 51]. Finally, we analyzed the impact of crowding on the performance of FRET-based glucose biosensors, equipped with FP-derivatives as FRET pair. Although this sensor is designed to respond to ligand binding with a conformational change, it shows also pronounced crowding induced conformational changes. In the case investigated here, glucose binding as well as the presence of macromolecular crowders lead to a structural compaction of the sensor construct, which both alters the FRET-ratio. The crowder-induced sensor compaction only takes place if macromolecular crowders (PEG and Ficoll with a few up to a few tens of kDa mass[46]) are used, whereas a compaction in the presence of small crowder agents (e.g. glycerol) was not observed. Importantly, the sensor sensitivity (given in reasonable large ΔR-values) is at least maintained under crowding conditions. However, the sensors would need an adapted calibration under equivalent crowding conditions, if employed under typical target conditions. The latter is challenging, specifically if such sensors are used intracellularily. In summary, we can state that synthetic polymer crowders can mimic already some properties of cellular crowding quite well, but it can be speculated that mixtures of multiple crowder agent components (also with more rigid crowder macromolecules, like double stranded DNA or proteins) may give even more convincing results[43].

ASSOCIATED CONTENT

Supporting Information. The Supporting Information is available free of charge on the ACS Publications website at DOI: xxxxxx.xxxx**.** Presentation of additional figures and tables.

AUTHOR INFORMATION

Corresponding Author

* fitter@physik.rwth-aachen.de; phone.: +49 241 8027209

ORCID

Jörg Fitter: 0000-0002-4503-2079

Henning Höfig: 0000-0003-0506-783X

Alexandros Katranidis: 0000-0002-1785-1659

Niklas O. Junker: 0000-0001-7586-9454

Martina Pohl: 0000-0001-9935-5183

Simone Wiegand: 0000-0001-6333-1956

AUTHOR CONTRIBUTIONS

J.F., N.J., and M.P. conceived the idea and designed the experiments. H.H., A.A., D.K., M.P., S.W., F.V., A.K. and N.J. performed and supervised the experiments. J.F., H.H., M.P., and S.W. wrote the manuscript with input from all authors.

ACKNOWLEDGEMENTS

The authors would like to thank our former Bachelor students for supporting us by determining bulk viscosities of various crowder solutions, by related FCS analyses (Birgit Hillebrecht, Friedmann Landmesser, Sabrina Smyczek, and Miraim Borgelt), and for measurements of the glucose binding curves (Tanja Schieck). H.H. acknowledges the International Helmholtz Research School on Biophysics and Soft Matter (BioSoft) for financial support.

REFERENCES

[1] Zimmerman, S. B., and Minton, A. P. (1993) Macromolecular Crowding - Biochemical, Biophysical, and Physiological Consequences, *Annual Review of Biophysics and Biomolecular Structure 22*, 27-65.

[2] Ellis, R. J. (2001) Macromolecular crowding: obvious but underappreciated, *Trends Biochem.Sci. 26*, 597-604.

[3] Schreiber, G., Haran, G., and Zhou, H. X. (2009) Fundamental Aspects of Protein-Protein Association Kinetics, *Chemical Reviews 109*, 839-860.

[4] Hall, D., and Minton, A. P. (2003) Macromolecular crowding: qualitative and semiquantitative successes, quantitative challenges, *Biochim Biophys Acta 1649*, 127-139.

[5] Verkman, A. S. (2002) Solute and macromolecule diffusion in cellular aqueous compartments, *Trends Biochem Sci 27*, 27-33.

[6] Mika, J. T., and Poolman, B. (2011) Macromolecule diffusion and confinement in prokaryotic cells, *Curr Opin Biotechnol 22*, 117-126.

[7] Zhou, H.-X. (2013) Influence of crowded cellular environments on protein folding, binding, and oligomerization: biological consequences and potentials of atomistic modeling, *FEBS letters 587*, 1053-1061.

[8] Zhou, H. X., Rivas, G., and Minton, A. P. (2008) Macromolecular crowding and confinement: biochemical, biophysical, and potential physiological consequences, *Annu Rev Biophys 37*, 375-397.

[9] Schavemaker, P. E., Boersma, A. J., and Poolman, B. (2018) How Important Is Protein Diffusion in Prokaryotes?, *Front Mol Biosci 5*, 93.

[10] Tabaka, M., Kalwarczyk, T., Szymanski, J., Hou, S., and Holyst, R. (2014) The effect of macromolecular crowding on mobility of biomolecules, association kinetics, and gene expression in living cells, *Frontiers in Physics 2*.

[11] Phillip, Y., and Schreiber, G. (2013) Formation of protein complexes in crowded environments - From in vitro to in vivo, *Febs Letters 587*, 1046-1052.

[12] Muramatsu, N., and Minton, A. P. (1988) Tracer diffusion of globular proteins in concentrated protein solutions, *Proc Natl Acad Sci U S A 85*, 2984-2988.

[13] Banks, D. S., and Fradin, C. (2005) Anomalous diffusion of proteins due to molecular crowding, *Biophysical Journal 89*, 2960-2971.

[14] Kuttner, Y. Y., Kozer, N., Segal, E., Schreiber, G., and Haran, G. (2005) Separating the contribution of translational and rotational diffusion to protein association, *J Am Chem Soc 127*, 15138-15144.

[15] Lavalette, D., Hink, M. A., Tourbez, M., Tetreau, C., and Visser, A. J. (2006) Proteins as micro viscosimeters: Brownian motion revisited, *European Biophysics Journal with Biophysics Letters 35*, 517-522.

[16] Zorrilla, S., Hink, M. A., Visser, A. J., and Lillo, M. P. (2007) Translational and rotational motions of proteins in a protein crowded environment, *Biophys.Chem. 125*, 298-305.

[17] Wang, Y., Li, C., and Pielak, G. J. (2010) Effects of proteins on protein diffusion, *J Am Chem Soc 132*, 9392-9397.

[18] Kalwarczyk, T., Ziebacz, N., Bielejewska, A., Zaboklicka, E., Koynov, K., Szymanski, J., Wilk, A., Patkowski, A., Gapinski, J., Butt, H. J., and Holyst, R. (2011) Comparative Analysis of Viscosity of Complex Liquids and Cytoplasm of Mammalian Cells at the Nanoscale, *Nano Letters 11*, 2157-2163.

[19] Zorrilla, S., and Lillo, M. P. (2009) Quantitative Investigation of Biomolecular Interactions in Crowded Media by Fluorescence Spectroscopy, a Good Choice, *Current Protein & Peptide Science 10*, 376-387.

[20] Dauty, E., and Verkman, A. S. (2004) Molecular crowding reduces to a similar extent the diffusion of small solutes and macromolecules: measurement by fluorescence correlation spectroscopy, *Journal of Molecular Recognition 17*, 441-447.
[21] Li, C., Wang, Y., and Pielak, G. J. (2009) Translational and rotational diffusion of a small globular protein under crowded conditions, *J Phys Chem B 113*, 13390-13392.
[22] Kumar, M., Mommer, M. S., and Sourjik, V. (2010) Mobility of cytoplasmic, membrane, and DNA-binding proteins in Escherichia coli, *Biophys J 98*, 552-559.
[23] Enderlein, J., Gregor, I., Patra, D., and Fitter, J. (2004) Art and artefacts of fluorescence correlation spectroscopy, *Curr.Pharm.Biotechnol. 5*, 155-161.
[24] Kempe, D., Cerminara, M., Poblete, S., Schone, A., Gabba, M., and Fitter, J. (2017) Single-Molecule FRET Measurements in Additive-Enriched Aqueous Solutions, *Analytical Chemistry 89*, 694-702.
[25] Bakshi, S., Siryaporn, A., Goulian, M., and Weisshaar, J. C. (2012) Superresolution imaging of ribosomes and RNA polymerase in live Escherichia coli cells, *Mol Microbiol 85*, 21-38.
[26] Mika, J. T., van den Bogaart, G., Veenhoff, L., Krasnikov, V., and Poolman, B. (2010) Molecular sieving properties of the cytoplasm of Escherichia coli and consequences of osmotic stress, *Mol Microbiol 77*, 200-207.
[27] Okumoto, S., Jones, A., and Frommer, W. B. (2012) Quantitative Imaging with Fluorescent Biosensors, *Annual Review of Plant Biology, Vol 63 63*, 663-706.
[28] Boersma, A. J., Zuhorn, I. S., and Poolman, B. (2015) A sensor for quantification of macromolecular crowding in living cells, *Nature Methods 12*, 227-+.
[29] Moussa, R., Baierl, A., Steffen, V., Kubitzki, T., Wiechert, W., and Pohl, M. (2014) An evaluation of genetically encoded FRET-based biosensors for quantitative metabolite analyses in vivo, *Journal of Biotechnology 191*, 250-259.
[30] Devanand, K., and Selser, J. C. (1991) Asymptotic-Behavior and Long-Range Interactions in Aqueous-Solutions of Poly(Ethylene Oxide), *Macromolecules 24*, 5943-5947.
[31] Kuznetsova, I. M., Turoverov, K. K., and Uversky, V. N. (2014) What Macromolecular Crowding Can Do to a Protein, *International Journal of Molecular Sciences 15*, 23090-23140.
[32] Groen, J., Foschepoth, D., te Brinke, E., Boersma, A. J., Imamura, H., Rivas, G., Heus, H. A., and Huck, W. T. S. (2015) Associative Interactions in Crowded Solutions of Biopolymers Counteract Depletion Effects, *J Am Chem Soc 137*, 13041-13048.
[33] Sadoine, M., Cerminara, M., Kempf, N., Gerrits, M., Fitter, J., and Katranidis, A. (2017) Selective Double-Labeling of Cell-Free Synthesized Proteins for More Accurate smFRET Studies, *Analytical Chemistry 89*, 11278-11285.
[34] Kempf, N., Remes, C., Ledesch, R., Zuchner, T., Höfig, H., Ritter, I., Katranidis, A., and Fitter, J. (2017) A Novel Method to Evaluate Ribosomal Performance in Cell-Free Protein Synthesis Systems, *Scientific Reports 7*, 467535.
[35] Höfig, H., Gabba, M., Poblete, S., Kempe, D., and Fitter, J. (2014) Inter-Dye Distance Distributions Studied by a Combination of Single-Molecule FRET-Filtered Lifetime Measurements and a Weighted Accessible Volume (wAV) Algorithm, *Molecules 19*, 19269-19291.
[36] Deuschle, K., Okumoto, S., Fehr, M., Looger, L. L., Kozhukh, L., and Frommer, W. B. (2005) Construction and optimization of a family of genetically encoded metabolite sensors by semirational protein engineering, *Protein Science 14*, 2304-2314.
[37] Steffen, V., Otten, J., Engelmann, S., Radek, A., Limberg, M., Koenig, B. W., Noack, S., Wiechert, W., and Pohl, M. (2016) A Toolbox of Genetically Encoded FRET-Based Biosensors for Rapid L-Lysine Analysis, *Sensors 16*.
[38] Lamprou, P., Kempe, D., Katranidis, A., Buldt, G., and Fitter, J. (2014) Nanosecond dynamics of calmodulin and ribosome-bound nascent chains studied by time-resolved fluorescence anisotropy, *Chembiochem : a European journal of chemical biology 15*, 977-985.

[39] Langevin, D., and Rondelez, F. (1978) Sedimentation of Large Colloidal Particles through Semidilute Polymer-Solutions, *Polymer 19*, 875-882.
[40] Zettl, U., Hoffmann, S. T., Koberling, F., Krausch, G., Enderlein, J., Harnau, L., and Ballauff, M. (2009) Self-Diffusion and Cooperative Diffusion in Semidilute Polymer Solutions As Measured by Fluorescence Correlation Spectroscopy, *Macromolecules 42*, 9537-9547.
[41] Kang, H., Pincus, P. A., Hyeon, C., and Thirumalai, D. (2015) Effects of macromolecular crowding on the collapse of biopolymers, *Phys Rev Lett 114*, 068303.
[42] Holyst, R., Bielejewska, A., Szymanski, J., Wilk, A., Patkowski, A., Gapinski, J., Zywocinski, A., Kalwarczyk, T., Kalwarczyk, E., Tabaka, M., Ziebacz, N., and Wieczorek, S. A. (2009) Scaling form of viscosity at all length-scales in poly(ethylene glycol) solutions studied by fluorescence correlation spectroscopy and capillary electrophoresis, *Physical Chemistry Chemical Physics 11*, 9025-9032.
[43] Biswas, S., Kundu, J., Mukherjee, S. K., and Chowdhury, P. K. (2018) Mixed Macromolecular Crowding: A Protein and Solvent Perspective, *Acs Omega 3*, 4316-4330.
[44] Liu, B. Q., Aberg, C., van Eerden, F. J., Marrink, S. J., Poolman, B., and Boersma, A. J. (2017) Design and Properties of Genetically Encoded Probes for Sensing Macromolecular Crowding, *Biophysical Journal 112*, 1929-1939.
[45] Gnutt, D., Gao, M., Brylski, O., Heyden, M., and Ebbinghaus, S. (2015) Excluded-Volume Effects in Living Cells, *Angewandte Chemie-International Edition 54*, 2548-2551.
[46] Höfig, H., Cerminara, M., Ritter, I., Schone, A., Pohl, M., Steffen, V., Walter, J., Vergara Dal Pont, I., Katranidis, A., and Fitter, J. (2018) Single-Molecule Studies on a FRET Biosensor: Lessons from a Comparison of Fluorescent Protein Equipped versus Dye-Labeled Species, *Molecules (Basel, Switzerland) 23*.
[47] Höfig, H., Otten, J., Steffen, V., Pohl, M., Boersma, A. J., and Fitter, J. (2018) Genetically Encoded Forster Resonance Energy Transfer-Based Biosensors Studied on the Single-Molecule Level, *ACS sensors 3*, 1462-1470.
[48] Gupta, S., Biehl, R., Sill, C., Allgaier, J., Sharp, M., Ohl, M., and Richter, D. (2016) Protein Entrapment in Polymeric Mesh: Diffusion in Crowded Environment with Fast Process on Short Scales, *Macromolecules 49*, 1941-1949.
[49] Kapanidis, A. N., Uphoff, S., and Stracy, M. (2018) Understanding Protein Mobility in Bacteria by Tracking Single Molecules, *J Mol Biol 430*, 4443-4455.
[50] Zimmerman, S. B., and Trach, S. O. (1988) Effects of macromolecular crowding on the association of E. coli ribosomal particles, *Nucleic Acids Res 16*, 6309-6326.
[51] Ge, X., Luo, D., and Xu, J. (2011) Cell-free protein expression under macromolecular crowding conditions, *PLoS One 6*, e28707.

TOC Graphic

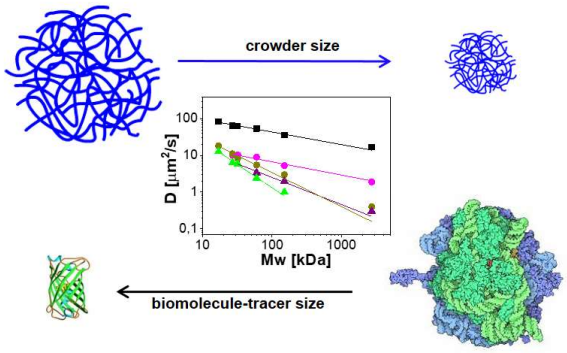
crowder size
100
10
1
0,1
D [μm²/s]
10
100
1000
Mw [kDa]
biomolecule-tracer size